Supplemental Material for

Enhanced fatigue resistance and lattice dynamics induced by the strong local strain in Fe-doped $KTa_{1-x}Nb_xO_3$ single crystal

Xiaolin Huang,[a] Peng Tan,*[ad] Yu Wang,[a] Yao Zhang,[a] Xiangda Meng, [a] Chengpeng Hu,[a] Guanchao Wang,[a] Zhongxiang Zhou [a] and Hao Tian*[abcd]

[a] School of Physics, Harbin Institute of Technology, Harbin 150001, China

[b] Key Laboratory of Micro-Nano Optoelectronic Information System, Ministry of Industry and Information Technology, Harbin 150001, China

[c] Collaborative Innovation Center of Extreme Optics, Shanxi University, Taiyuan, Shanxi 030006, China

[d] Heilongjiang Provincial Key Laboratory of Plasma Physics and Application Technology, Harbin 150001, China

* Corresponding Author: tanpeng@hit.edu.cn and tianhao@hit.edu.cn

Experimental Details.

The raw materials of potassium carbonate (K_2CO_3, 99.99%), tantalum pentoxide (Ta_2O_5, 99.99%), niobium pentoxide (Nb_2O5, 99.99%) and ferric oxide (Fe_2O_3, 99.99%) powders were weighed according to the phase diagram. The mole ratio of K_2CO_3, Ta_2O_5, Nb_2O_5 and Fe_2O_3 was 1.04: 0.50: 0.50: 0.005, and an excess K_2CO_3 was added as a self-flux to decrease the growth temperature. The mixed powders in ethanol were ball-milled for 24 h. Then, the dried powders were put into a platinum crucible and calcined at 900℃ to get the KTN compound. The compound was melted at 1300℃, and was lifted at the crystallization temperature according to the phase diagram to get the single crystals.

The polarization-electric field hysteresis (*P*-*E*) loops of Fe-KTN and pristine KTN were measured at 50 Hz under different electric fields (from 2.0 kV cm^{-1} to 15.0 kV cm^{-1}). The *S*-*E* of these single crystals were also measured at 15kV cm^{-1}. To characterize fatigue properties, the cyclic electric field (12 kV cm^{-1} at 100 Hz) was applied, and the number of cycles increased from 10^2 to 10^5. The current density (*J*-*E*) curves of samples under different electric fields were obtained at 50 Hz.

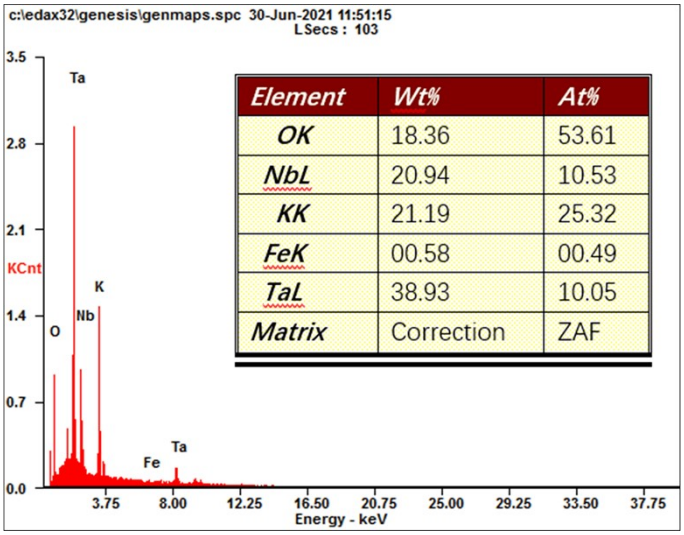

Element	Wt%	At%
OK	18.36	53.61
NbL	20.94	10.53
KK	21.19	25.32
FeK	00.58	00.49
TaL	38.93	10.05
Matrix	Correction	ZAF

Figure S1. The element atomic percentages of Fe-doped KTN

The Fe element atomic percentage is similar to the mole ratio (0.5% mol) we designed.

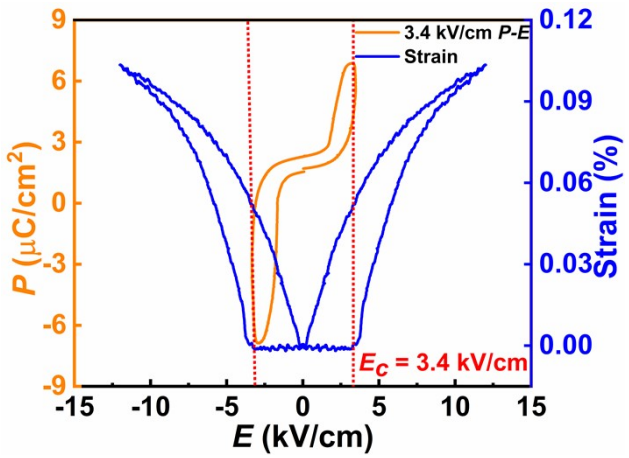

Figure S2. The double hysteresis loop at E_c and the electric-field-induced strain at 12 kV cm^{-1}.

When the electric field is larger than 3.4 kV cm^{-1}, the polarization of the hysteresis loop changes significantly as shown in Figure S2. It suggests that the coercive field (E_c) of the crystal is 3.4 kV cm^{-1}. In addition, the electric-field-induced strain at 12 kV cm^{-1} is shown. The switching of the non-180° domain structures also proves that the E_c of the tetragonal Fe-KTN is 3.4 kV cm^{-1}

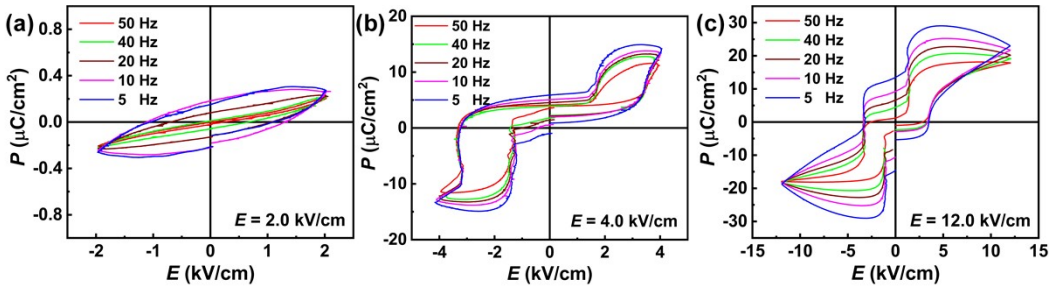

Figure S3. The variable-frequency *P-E* loops of the Fe-KTN single crystals under different electric fields, (a) $E = 2.0$ kV cm^{-1}, (b) $E = 4.0$ kV cm^{-1}, (c) $E = 12.0$ kV cm^{-1}

The scaling relation of the energy dissipation is expressed as $< A > \propto f^{\alpha} E^{\beta}$. Here, we calculate the logarithm of the scaling relation to obtain the α by fitting, $\ln(< A >) \propto \alpha \ln(f)$. Based on the variable-frequency *P-E* loops of the Fe-KTN single crystals (Figure S3), we calculated the the hysteresis area (<*A*>) and the accurate α of Fe-KTN under different *E*. The same calculation was applied to the pristine KTN.

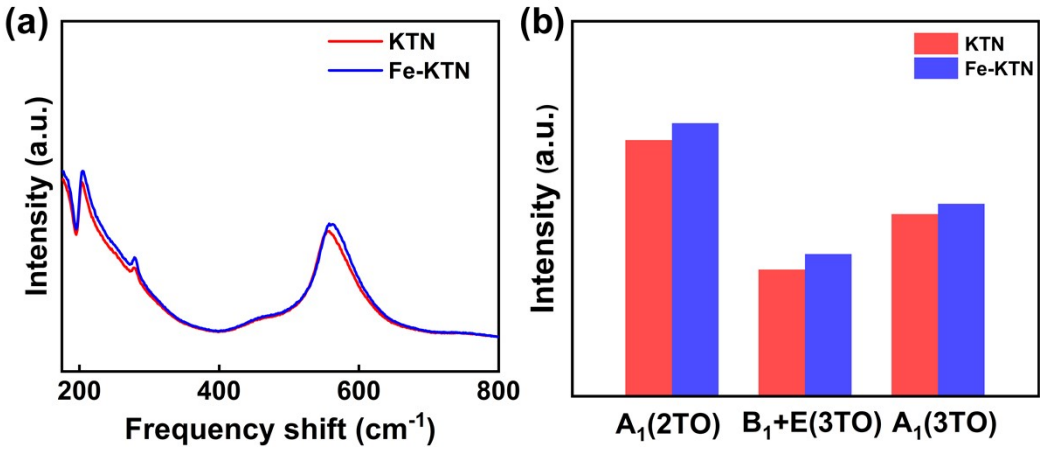

Figure S4. (a) The normalized Raman spectra from 175 cm^{-1} to 800 cm^{-1}. (b) The Raman intensity of each lattice vibration mode in Fe-KTN and KTN.

The intensities of the three typical lattice vibration modes in Fe-KTN are larger than these of pristine KTN.

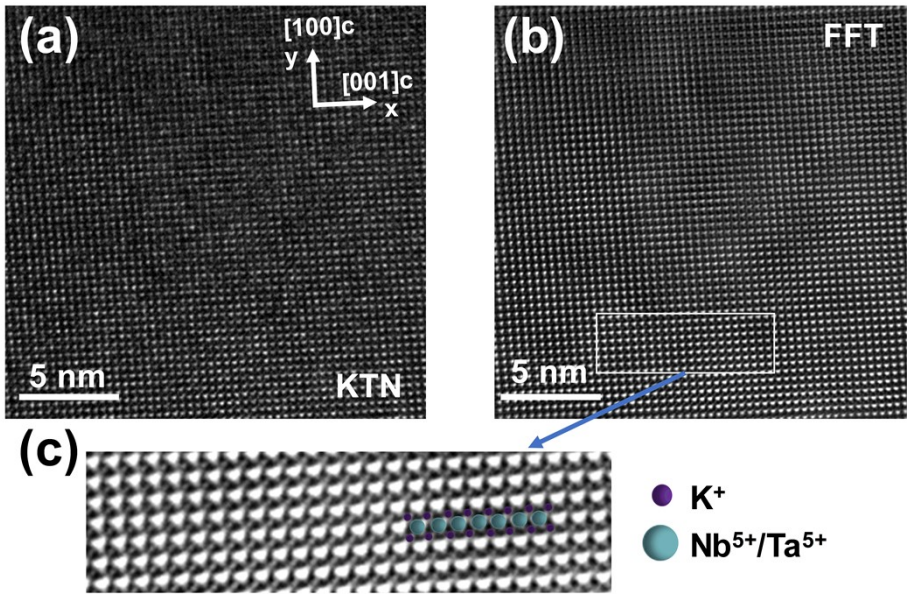

Figure S5. The HRTEM image of pristine KTN (a) and the corresponding image of atomic distribution after FFT (b). (c) The part of atomic distribution after zooming. The center arrangement of the B-site ions is pointed in pristine KTN.

The microscopic atomic arrangement of pristine KTN single crystals along the direction of $(010)_c$ is shown in Figure S5(a). The image after fast Fourier transform (FFT) is exhibited as the Figure 5(b), and the part of atomic distribution is shown in Figure S5(c) after zooming. The B-site ions are located at the center of the four adjacent K^+ ions. The angle of three non-adjacent K^+ ions inside KTN is 88.836°.

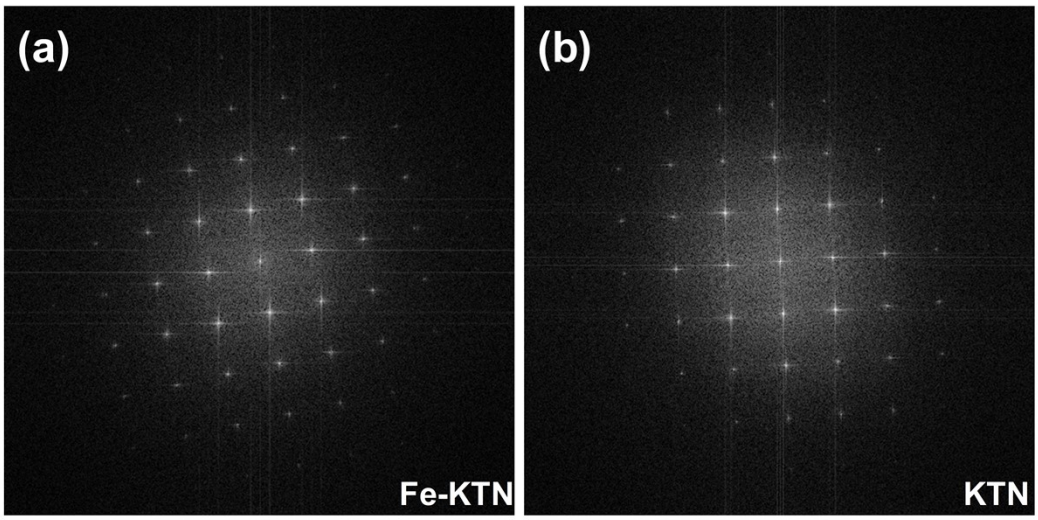

Figure S6. The typical diffraction patterns of bright-field HRTEM in Fe-KTN (a) and pristine KTN (b).

Figure S6 exhibits the bright-field diffraction patterns of Fe-KTN and KTN, which indicates our as-grown single crystals are in the tetragonal phase at room temperature.

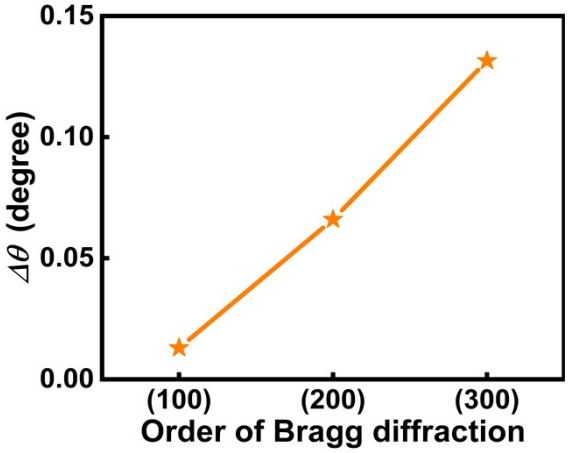

Figure S7. The difference between the angles of the diffraction peaks of Fe-KTN and KTN.

Table S1. The element atomic percentages of Fe-doped KTN and pristine KTN single crystal

	K(mol%)	O(mol%)	Ta(mol%)	Nb(mol%)	Fe(mol%)	Ta/Nb
Fe-KTN	25.32	53.61	10.05	10.53	0.49	0.95
Pristine KTN	25.85	52.64	10.66	10.85	-	0.98

Table S2. The angles of diffraction peaks (300) and the lattice parameters of Fe-KTN and KTN.

	$2\theta_a$	$2\theta_c$	$a = b$ (Å)	c (Å)
Fe-KTN	70.84°	70.56°	3.987	4.001
Pristine KTN	70.78°	70.52°	3.990	4.003

The lattice parameters of Fe-KTN are less than these of KTN, which indicates the bond length inside Fe-KTN becomes shorter than that in KTN after Fe doping. Experimentally, the lattice contraction happens in Fe-KTN single crystals.